# RESEARCH PAPERS

*Acta Cryst.* (1995). A**51**, 253–258

## The Dispersion Surface of X-rays Very Near the Absorption Edge

BY TOMOE FUKAMACHI AND RIICHIROU NEGISHI

*Saitama Institute of Technology, Okabe, Saitama* 369-02, *Japan*

AND TAKAAKI KAWAMURA

*Department of Physics, Yamanashi University, Kofu, Yamanashi* 400, *Japan*

(*Received* 26 *May* 1994; *accepted* 13 *September* 1994)

### Abstract

To discuss the X-ray dynamical diffraction when the imaginary part of the X-ray polarizability is larger than the real part, the dispersion surface is studied as a function of the ratio between the real and the imaginary parts of the polarizability. The dispersion surface in the Laue case when the real part is zero has a similar form to that in the Bragg case when the imaginary part is zero. The relations between the dispersion surface and the diffracted intensity are studied in some special cases. The abnormal absorption and the abnormal transmission effect are related to the features of the dispersion surface.

### 1. Introduction

By using X-rays from synchrotron radiation, it is possible to study dynamical diffraction very near the absorption edge of an atom in a crystal. The real and imaginary parts of the X-ray polarizability can be changed by tuning the X-ray energy. In an extreme case, the diffraction can be observed when the real part of the X-ray polarizability is zero. Fukamachi *et al.* (1993) observed the dynamical diffraction for high-order reflections from Ge when the real part was zero.

Up to now, most dynamical diffractions have been studied when the imaginary part of the X-ray polarizability is much smaller than the real part. The theories (Zachariasen, 1945; James, 1963; Miyake, 1969; Pinsker, 1978) for treating the diffraction in such a case is not applicable when the real part is zero. Recently, Fukamachi & Kawamura (1993) (hereinafter referred to as FK) revised the dynamical theory to treat the diffraction regardless of the values of the real and imaginary parts. They discussed the diffracted and the transmitted intensities when the real part is zero. In the dynamical theory, it is useful to study the dispersion surfaces in order to understand the geometry in the wave-number space. In this paper, the dispersion surface and the corresponding rocking curves are studied for several ratios between the real and imaginary parts of the X-ray polarizability.

### 2. Equation of dispersion surface

We define the Fourier transforms of the real and imaginary parts of the X-ray polarizability as $\chi_h^r$ and $\chi_h^i$, respectively. The Fourier transform of the polarizability is given by

$$\chi_h = \chi_h^r + i\chi_h^i = |\chi_h^r| \exp(i\alpha_h^r) + i|\chi_h^i| \exp(i\alpha_h^i). \quad (1)$$

Here **h** is a reciprocal-lattice vector, $\alpha_h^r$ and $\alpha_h^i$ are the phases of $\chi_h^r$ and $\chi_h^i$, respectively. According to FK, we define $\bar{\chi}_h$ as

$$\bar{\chi}_h = (|\chi_h^r|^2 + |\chi_h^i|^2)^{1/2}, \quad (2)$$

then we have the relation

$$\chi_h \chi_{-h} = \bar{\chi}_h^2 (1 - b^2 + i\,2p \cos\delta). \quad (3)$$

Here, the parameters $b$, $p$ and $\delta$ are given by

$$b = (2q)^{1/2} \quad (4)$$

$$p = |\chi_h^r||\chi_h^i|/\bar{\chi}_h^2 = (|\chi_h^r|/|\chi_h^i|)q \quad (5)$$

and

$$\delta = \alpha_h^i - \alpha_h^r \quad (6)$$

by using the parameter $q$,

$$q = 1/(1 + |\chi_h^r|^2/|\chi_h^i|^2). \quad (7)$$

The parameter $q$ is zero for $|\chi_h^i| = 0$, 0.5 for $|\chi_h^r| = |\chi_h^i|$ and 1 for $|\chi_h^r| = 0$. The values of $b$, $p$ and $\chi_h\chi_{-h}$ for $q = 0$, 0.5 and 1 are listed in Table 1.

By defining the real and imaginary parts of the wave vector of the incident beam in a crystal, $\kappa_0$, as

$$\boldsymbol{\kappa}_0 = \boldsymbol{\kappa}_{0r} + i\boldsymbol{\kappa}_{0i}, \quad (8)$$

we have the relations

$$|\boldsymbol{\kappa}_{0r}| = \kappa_{0r} = K(1 + \chi_0^r/2) \quad (9)$$

and

$$\kappa_{0i} = |\boldsymbol{\kappa}_{0r}|\chi_0^i/2 = \kappa_{0r}\chi_0^i/2 \simeq K\chi_0^i/2. \quad (10)$$

The wave number $K$ is the magnitude of the incident wave vector in vacuum. The linear absorption coefficient is given by

$$\mu = -2\pi K \chi_0^i. \tag{11}$$

For $\sigma$ polarization, the equation of the dispersion surface is expressed by

$$(\xi_0 - i\kappa_{0i})(\xi_h - i\kappa_{0i}) = \kappa_{0r}^2 \bar{\chi}_h^2 (1 - b^2 + 2ip\cos\delta)/4, \tag{12}$$

where the parameters $\xi_0$ and $\xi_h$ are defined as

$$\xi_0 - i\kappa_{0i} = \mathbf{k}_0 - \boldsymbol{\kappa}_0 \tag{13}$$

and

$$\xi_h - i\kappa_{0i} = \mathbf{k}_h - \boldsymbol{\kappa}_0. \tag{14}$$

Here, we use the two-wave approximation. Owing to diffraction, the wave vector of the incident beam becomes $\mathbf{k}_0$ so as to satisfy (12) and $\mathbf{k}_h$ is the corresponding wave vector for the diffracted beam. If we take the $X$ axis parallel to the surface and the $Y$ axis outward normal to it, we have relations

$$\begin{aligned} \xi_0 &= \mathbf{i}X\sin\theta_1 + \mathbf{j}Y\cos\theta_1 \\ \xi_h &= \mathbf{i}X\sin\theta_2 + \mathbf{j}Y\cos\theta_2. \end{aligned} \tag{15}$$

The unit vector in the $X$ direction is $\mathbf{i}$ and that in the $Y$ direction is $\mathbf{j}$. The geometrical illustration is shown in Fig. 1 for when the imaginary part of the polarizability is zero ($q = 0$). The angles $\theta_1$ and $\theta_2$ are also shown in Fig. 1.

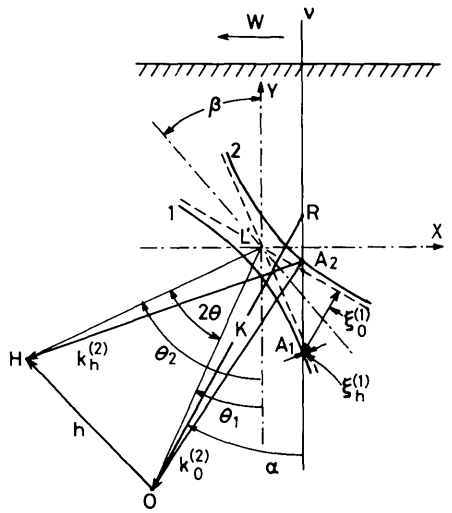


Fig. 1. The schematic diagram of the diffraction condition and the dispersion surface near a Bragg condition. 0: the incident point; $H$: the diffraction point; $\mathbf{h}$: the reciprocal-lattice vector; $\theta$: Bragg angle; $A_1$ and $A_2$: the dispersion points on branches 1 and 2; $v$: surface normal.

Table 1. *Values of parameters for three conditions between $\chi_h^r$ and $\chi_h^i$*

| Condition | $q$ | $b$ | $p$ | $\chi_h\chi_{-h}$ |
|---|---|---|---|---|
| $\chi_h^i = 0$ | 0 | 0 | 0 | $\lvert\chi_h^r\rvert^2$ |
| $\lvert\chi_h^r\rvert = \lvert\chi_h^i\rvert$ | 1/2 | 1 | 1/2 | $i\bar{\chi}_h^2\cos\delta$ |
| $\chi_h^r = 0$ | 1 | $2^{1/2}$ | 0 | $-\lvert\chi_h^i\rvert^2$ |

It is convenient to define a parameter called 'resonance error' $W$ as

$$W = -X\sin 2\theta/(|\cos\theta_1\cos\theta_2|^{1/2}\kappa_{0r}\bar{\chi}_h). \tag{16}$$

As shown in Fig. 1, $\theta$ is the Bragg angle. By inserting (15) into (12), we obtain

$$\begin{aligned} Y = (\pm)\kappa_{0r}\bar{\chi}_h/(2|\cos\theta_1\cos\theta_2|)^{1/2}\{&(\sin 2\beta/\sin 2\theta)W \\ &+ ig\cos\theta\sin\beta/|\cos\theta_1\cos\theta_2|^{1/2} \pm [(W + ig')^2 \\ &(\pm)(1 - b^2 + 2ip\cos\delta)]^{1/2}\}. \end{aligned} \tag{17}$$

The parameters $g$ and $g'$ are defined as

$$g = g_0 q^{1/2} \tag{18}$$

and

$$g' = g\sin\theta\cos\beta/(|\cos\theta_1\cos\theta_2|^{1/2}\kappa_{0r}\bar{\chi}_h), \tag{19}$$

where $g_0 = \chi_0^i/|\chi_h^i|$ and the angle $\beta$ is given in Fig. 1. For the double signs ($\pm$) in (17), the positive sign is taken for the Laue case ($\cos\theta_2 > 0$) and the negative sign for the Bragg case ($\cos\theta_2 < 0$). In the following, we consider only the symmetric Laue and the symmetric Bragg cases for $\sigma$ polarization. For $\pi$ polarization, we obtain similar formulae by multiplying the polarization factor $|\cos 2\theta|$ with $\chi_h^r$ and $\chi_h^i$.

## 3. Symmetric Laue case

In the symmetric Laue case, $\beta = \pi/2$ and $\theta = -\theta_1 = \theta_2$. The difference between the two solutions $Y^{(1)}$ and $Y^{(2)}$ of (17), which is the distance between two dispersion points, is

$$Y^{(2)} - Y^{(1)} = (s/\pi)L^{1/2}. \tag{20}$$

Here, $s$ and $L$ are

$$s = \pi\kappa_{0r}\bar{\chi}_h/\cos\theta \tag{21}$$

and

$$L = W^2 + 1 - b^2 + 2ip\cos\delta. \tag{22}$$

### 3.1. *In the case when $q = 0$*

When $q = 0$ (no absorption case), the equation of the dispersion surface becomes the well known form

$$(Y\cos\theta)^2 - (X\sin\theta)^2 = \kappa_{0r}^2|\chi_h^r|^2/4. \tag{23}$$

The dispersion surface is a hyperbola, as shown in Fig. 2(*a*). The rocking curve of the diffracted beam $P_h/P_0$, calculated for $sH = \pi$ and $\delta = 0$, is shown in Fig. 3(*a*) with $P_0$ and $P_h$ being the incident and diffracted intensities, respectively, and $H$ being the thickness of the crystal. To show the correspondence between the dispersion surface and the rocking curve, we take $-W$ as the abscissa in Fig. 3. Since there is a gap between two dispersion points, we have two wave numbers of slightly different values, which cause interference fringes known as the *Pendellösung* beat. When $sH = \pi$ the diffracted intensity is zero at $W = 0$.

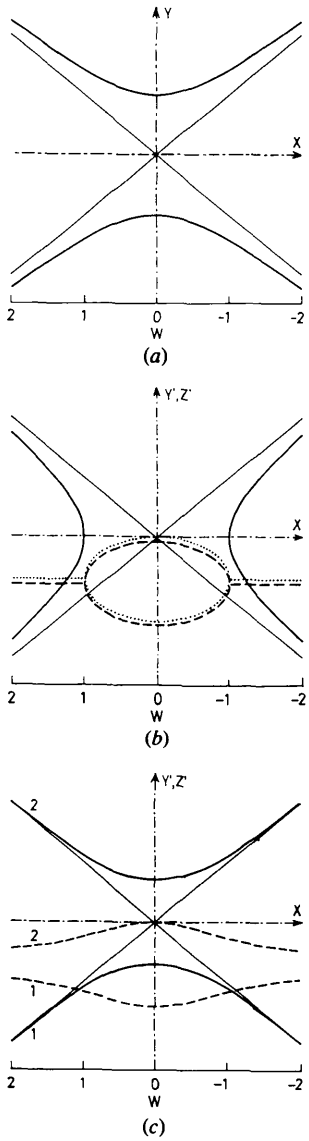


Fig. 2. The dispersion surfaces in the symmetric Laue case. The abscissa is the $-W$ axis. The solid and dashed curves are the real and imaginary parts of the curves. $\delta = 0$. (*a*) $q = 0$; (*b*) $q = 1$, $g_0 = -1.1$; (*c*) $q = 0.5$, $g_0 = -1$. The dotted curve in (*b*) shows the imaginary part for $q = 1$, $g_0 = -1$.

### 3.2. *In the case when* $q = 1$

When $q = 1$ (no real part of the polarizability), $b = 2^{1/2}$, $p = 0$ and the right-hand side of (12) is negative. Since the value of $Y$ in (17) is complex in general, we take

$$Y = Y' + iZ', \tag{24}$$

where $Y'$ and $Z'$ are both real. By substituting (15) and (24) into (12), we have

$$(Y'\cos\theta)^2 - (X\sin\theta)^2 - (Z'\cos\theta - \kappa_{0i})^2 = -\kappa_{0r}^3|\chi_h^i|^2/4 \tag{25}$$

and

$$Y'\cos\theta(Z'\cos\theta - \kappa_{0i}) = 0. \tag{26}$$

When $Y'\cos\theta = 0$, we have from (25)

$$(X\sin\theta)^2 + (Z'\cos\theta - \kappa_{0i})^2 = \kappa_{0r}^2|\chi_h^i|^2/4. \tag{27}$$

On the other hand, when $Z'\cos\theta - \kappa_{0i} = 0$, we have

$$(X\sin\theta)^2 - (Y'\cos\theta)^2 = \kappa_{0r}^2|\chi_h^i|^2/4. \tag{28}$$

The dispersion surfaces obtained from (27) and (28) are shown in Fig. 4. Equation (28) expresses a hyperbola in the plane $Z' = \kappa_{0i}/\cos\theta$. The value of $Z' = \kappa_{0i}/\cos\theta$ corresponds to the mean absorption because $2\pi Z'H$ is rewritten as $-\mu H/(2\cos\theta)$ in this case. If the right-hand side of (28) has the same value as that of (23), the two equations are conjugate. The dispersion surface of (28) is obtained by rotating that of (23) 90° clockwise.

Equation (27) expresses an ellipse in the plane of $Y = 0$ with one axis along $X = 0$ and the other along $Z' = \kappa_{0i}/\cos\theta$. The dispersion points in the complex

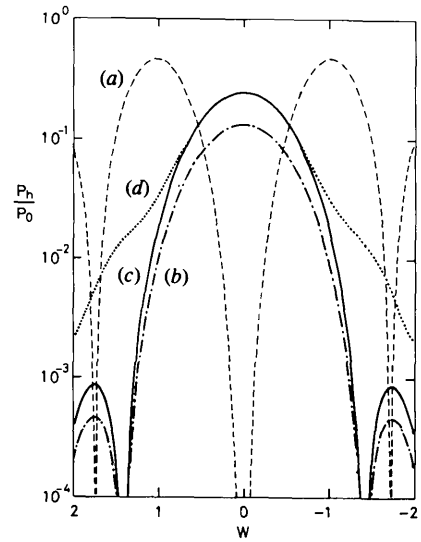


Fig. 3. The rocking curves in the symmetric Laue case for $\delta = 0$, $sH = \pi$. (*a*) $q = 0$; (*b*) $q = 1$, $g_0 = -1.1$; (*c*) $q = 1$, $g_0 = -1$; (*d*) $q = 0.5$, $g_0 = -1$.

plane are determined as intersecting points of the ellipse with $\nu'$ in the $XZ'$ plane that corresponds to the surface normal axis $\nu$. The form of the dispersion surface is quite similar to that in the Bragg case when the imaginary part of the polarizability is zero, which will be shown in the next section. The value of $|Z'|$ is minimum at $W = 0$ for the branch closer to $Z' = 0$ and is maximum at $W = 0$ for the branch further from $Z' = 0$. When $X$ is large enough, the two dispersion points are on the hyperbola on the right-hand side of Fig. 4. With decreasing $X$, the dispersion points are degenerate at a point $X = \kappa_{0r}|\chi_h^i|/(2\sin\theta)$, then leave the hyperbola. They are on the ellipse until they become degenerate at a point $X = -\kappa_{0r}|\chi_h^i|/(2\sin\theta)$, where they leave the ellipse and move to the other side of the hyperbola.

Fig. 2(*b*) shows the dispersion surface similar to Fig. 4 in a different way as a function of $W$. The ordinate is the $Z'$ axis as well as the $Y'$ axis. The solid curves are the hyperbola as in Fig. 4 and the dashed curves are the curves in the $Y' = 0$ plane in Fig. 4. The two dashed straight lines in Fig. 2(*b*) give the mean absorption. We have assumed $g_0 = -1.1$. The rocking curve in this case is shown in Fig. 3(*b*). At $W = 0$, the intensity becomes maximum due to abnormal transmission because $|Z'|$ is a minimum. When $|W| > 1$, $Z' = \kappa_{0i}/\cos\theta$ and $Y' \neq 0$, the *Pendellösung* beat is observed as a result of the interference between two branches of waves. Since $|g_0|$ is large ($g_0 = -1.1$), the intensity becomes extremely small for a thick crystal.

The imaginary part of the dispersion surface for $g_0 = -1$ is shown by the dotted line in Fig. 2(*b*). The real part is not shown because it is quite similar to that in Fig. 2(*b*). At $W = 0$, the dotted ellipse is tangential to the $Z' = 0$ line. The wave corresponding to this point does not show any absorption. This explains the abnormal transmission of 25% for both the transmitted and the diffracted intensities regardless of the thickness of the crystal, which is discussed by FK. The rocking curve in this case is shown in Fig. 3(*c*). It is noted that the intensity at $W = 0$ in (*c*) is higher than in (*b*).

### 3.3. *In the case when* $q = 0.5$

Fig. 2(*c*) shows the dispersion surface when $q = 0.5$ and $g_0 = -1.0$. The solid curves show the real part of the dispersion surface and the dashed curves show the imaginary part. The real and imaginary parts of branches 1 and 2 are denoted by the numbers. The real part (the solid curves) is quite similar to the dispersion surface in Fig. 2(*a*). For any $W$, there are two branch points of different imaginary parts (the dashed curves): one is always larger than the other. This results in different amplitudes of waves for branches 1 and 2 and the diffracted intensity in Fig. 3(*d*) does not become zero due to the interference. Since the imaginary part of branch 2 is tangential to the line $Z' = 0$ at $W = 0$, both the transmitted and diffracted intensities become 25% of the incident intensity for a thick crystal owing to the abnormal transmission effect. The wave of branch 1, on the other hand, suffers abnormal absorption at $W = 0$, twice as large as the normal absorption.

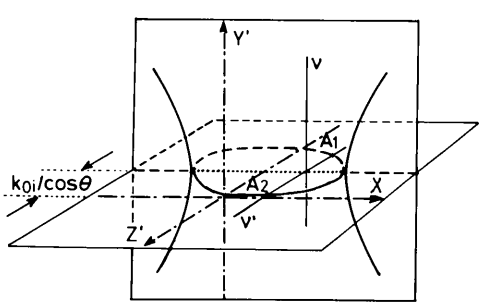


Fig. 4. The dispersion surface in the symmetric Laue case for $q = 1$. The conditions are the same as in Fig. 2(*b*).

## 4. Symmetric Bragg case

In the symmetric Bragg case, $\beta = 0$ and $\theta = \pi/2 - \theta_1 = \theta_2 - \pi/2$. The basic equation of the dispersion surface is written using (12) and (15),

$$(Y\sin\theta)^2 - (X\cos\theta - i\kappa_{0i})^2 = -\kappa_{0r}^2\bar{\chi}_h^2(1 - b^2 + 2ip\cos\delta)/4. \tag{29}$$

If we put $Y = Y' + iZ'$ ($Y', Z'$ real), we have

$$(Y'\sin\theta)^2 - (Z'\sin\theta)^2 - (X\cos\theta)^2 = -\kappa_{0i}^2 - \kappa_{0r}^2\bar{\chi}_h^2(1 - b^2)/4 \tag{30}$$

and

$$2Y'Z'\sin^2\theta = 2\kappa_{0i}X\cos\theta - \kappa_{0r}^2\bar{\chi}_h^2 p\cos\delta/2. \tag{31}$$

### 4.1. *In the case when* $q = 0$

When $q = 0$, parameters $b$ and $p$ are both zero. From (31), either $Y' = 0$ or $Z' = 0$. The equation of the dispersion surface for $Z' = 0$ is written as

$$(X\cos\theta)^2 - (Y'\sin\theta)^2 = \kappa_{0r}^2|\chi_h^r|^2/4; \tag{32}$$

for $Y' = 0$, it is written as

$$(X\cos\theta)^2 + (Z'\sin\theta)^2 = \kappa_{0r}^2|\chi_h^r|^2/4. \tag{33}$$

The dispersion surfaces obtained from (32) and (33) are shown in Fig. 5(*a*) as a function of $W$ in the same manner as in Fig. 2. The dispersion points are on the hyperbola (the solid curves) when $|W| > 1$ and on the ellipse (the dashed curve) when $|W| < 1$. At $|W| = 1$, the dispersion points are degenerate. The rocking curve of the diffracted beam from a semi-infinite crystal is of a top hat form as shown in Fig. 6(*a*). It is noted that (32) is similar to (28) in the Laue case and (33) is similar to (27). The dispersion surface, without the imaginary part of polarizability in the symmetric Bragg case, is rotated

90° from that in the symmetric Laue case, *i.e.* $\beta = 0$ in the Bragg case and $\beta = \pi/2$ in the Laue case. The dispersion surface, without real-part polarizability in the Laue case, is also rotated 90° from that without the imaginary part, as shown in Figs. 2(*a*) and (*b*). The dispersion surface in Fig. 5(*a*) is quite similar to that in Fig. 2(*b*). The upper half of the dashed curve gives rise to the enhancement of the wave into the crystal, which is not a realistic branch for a semi-infinite crystal.

### 4.2. *In the case when* $q = 1$

When $q = 1$, (30) becomes

$$(Y' \sin\theta)^2 - (Z' \sin\theta)^2 - (X \cos\theta)^2 = \kappa_{0r}^2 |\chi_h^i|^2 (1 - g^2)/4 \quad (34)$$

and (31) becomes

$$Y'Z' \sin^2\theta = \kappa_{0r} |\chi_h^i| g X \cos\theta/2. \quad (35)$$

The resonance error $W$ is written using $X$ as

$$W = -2X \cos\theta/(\kappa_{0r} |\chi_h^i|). \quad (36)$$

When $W = 0$, $Y'$ or $Z'$ must be zero according to (35). As examples, the dispersion surfaces for $g_0 = -1.2$ and $g_0 = -1$ are shown in Figs. 5(*b*) and (*c*), respectively. For $g_0 = -1.2$, $Y'$ is zero but $Z'$ is not zero at $W = 0$ ($X = 0$). For $g_0 = -1$, both $Y'$ and $Z'$ are zero at $W = 0$.

The rocking curves from a semi-infinite crystal corresponding to these dispersion surfaces are shown in Figs. 6(*b*) and (*c*). The curve (*c*) shows a sharp peak with the maximum intensity of 1 at $W = 0$, which corresponds to the point where $Y'$ and $Z'$ are both zero. Since there is no gap between the two hyperbolas (the solid curves) in (*c*), the curve does not have a top hat form and the width is quite small owing to rapid change of $Z'$ around $W = 0$. This sharp rocking curve has been pointed out by Kato (1992) and FK.

### 4.3. *In the cases when* $q = 0.5$ *and* 0.01

For $g_0 = -1$ and $q = 0.5$, the dispersion surface is shown in Fig. 5(*d*) and the rocking curve in Fig. 6(*d*). At a certain value of $W$ between $-1$ and 0, $Y'$ and $Z'$ both become zero, where the diffracted intensity shows maximum as shown in Fig. 6(*d*). The dispersion surface in Fig. 5(*d*) is not symmetric with respect to the line of $W = 0$, and the corresponding rocking curve [Fig. 6(*d*)] is not symmetric either.

For $g_0 = -1$ and $q = 0.01$, the dispersion surface is shown in Fig. 5(*e*) and the rocking curve in Fig. 6(*e*). At first sight, the curve looks quite different from that in Fig. 6(*a*), but it is noted that curve (*e*) becomes curve (*a*) in the limit of $q \to 0$ ($g \to 0$). In this limit, the dispersion surface in (*a*) is interpreted as follows. Branch 1 (the upper half of the left-hand side) and branch 2′ (the lower half of the right-hand side) are regarded as being realistic

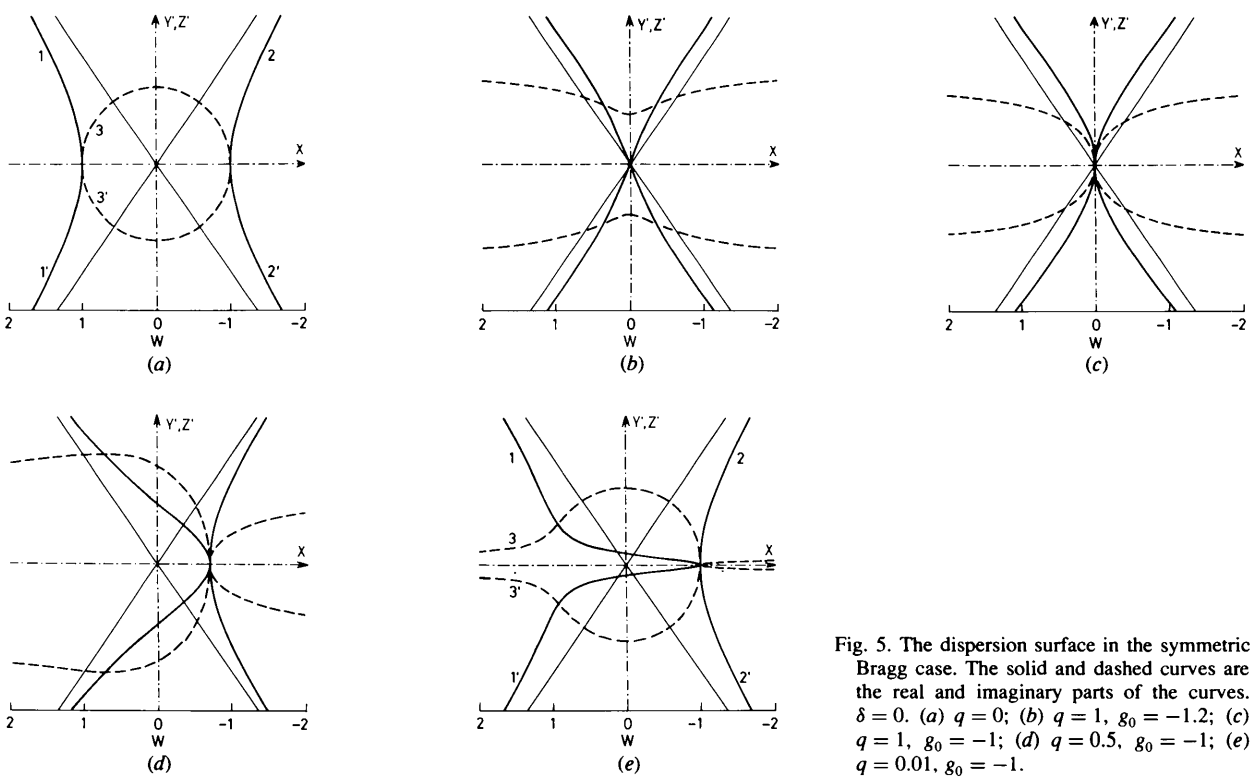


Fig. 5. The dispersion surface in the symmetric Bragg case. The solid and dashed curves are the real and imaginary parts of the curves. $\delta = 0$. (*a*) $q = 0$; (*b*) $q = 1$, $g_0 = -1.2$; (*c*) $q = 1$, $g_0 = -1$; (*d*) $q = 0.5$, $g_0 = -1$; (*e*) $q = 0.01$, $g_0 = -1$.

in the sense that the corresponding wave suffers absorption when it propagates into a semi-infinite crystal (Miyake, 1969). 1′ and 2 branches are not realistic because the corresponding wave suffers intensity enhancement in the crystal. The dashed curve 3 gives $Z' \geq 0$ and is unrealistic, so that the realistic branch starting from curve 1 for $W > 1$ leaves the hyperbola at $W = 1$ and follows the curve 3′. It leaves curve 3′ at $W = -1$ and follows the curve 2′. In a similar manner, in Fig. 5(*e*), for the realistic branch, the real part is given by curve 1 for $W > -1$ and by curve 2′ for $W < -1$. The imaginary part of the realistic branch always stays in the lower half of the dashed curve. If we compare the realistic branches in (*a*) and (*e*), they have a similar form. In Fig. 6(*e*), the diffracted intensity does not have a top-hat form and has the maximum near $W = -1$ when $Z' = 0$. The total reflection occurs at one point near $W = -1$.

## 5. Summary

We have studied dispersion surfaces by changing the ratio between the real and imaginary parts of the X-ray polarizability. It is shown that the dispersion surface in the symmetric Laue case for no real part of the polarizability ($q = 1$) is quite different from the well known form of the dispersion surface when the imaginary-part polarizability is zero. It shows a similar form to that in the symmetric Bragg case for no imaginary part of the polarizability. The dispersion surface in the Laue case for $q = 1$ becomes pure imaginary for $-1 < W < 1$, which explains why the abnormal transmission and absorption effects result.

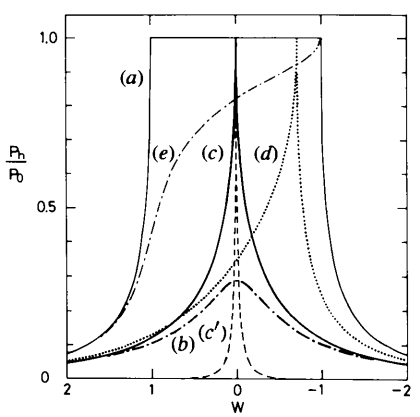


Fig. 6. The rocking curves in the symmetric Bragg case. The conditions for curves (*a*)–(*e*) correspond to those in Fig. 5. The details for curve (*c*′) are given in the text.

In the symmetric Bragg case from a semi-infinite crystal, the dispersion surface for no real part of the polarizability has no gap between the two branches and the two branches are tangential to each other at $W = 0$. This results in a very sharp rocking curve when the real-part polarizability is zero. The sharp rocking curve may be useful for a monochromator with small divergent angle. As an example, Fig. 6(*c*′) shows the rocking curve after four times diffraction from such a channel-cut monochromator. The width of the rocking curve (*c*′) is 1/100 of the curve (*a*).

As shown above, the complex dispersion surfaces for various values of $q$ are quite useful to interpret not only the shapes of the rocking curves but also the abnormal transmission and absorption effects. It is also possible to obtain information on the phases of waves corresponding to each branch point by using the dispersion surface. A paper on this topic will be published in the near future.

### References

FUKAMACHI, T. & KAWAMURA, T. (1993). *Acta Cryst.* A**49**, 384–388.
FUKAMACHI, T., NEGISHI, R., YOSHIZAWA, M., EHARA, K., KAWAMURA, T., NAKAJIMA, T. & ZHAO, Z. (1993). *Acta Cryst.* A**49**, 573–575.
JAMES, R. W. (1963). *Solid State Phys.* **15**, 53–220.
KATO, N. (1992). *Acta Cryst.* A**48**, 829–833.
MIYAKE, S. (1969). *X-ray Diffraction*. Tokyo: Asakura. (In Japanese.)
PINSKER, Z. G. (1978). *Dynamical Scattering of X-rays in Crystals*. New York: Springer.
ZACHARIASEN, W. H. (1945). *Theory of X-ray Diffraction in Crystals*. New York: Dover.

*Acta Cryst.* (1995). A**51**, 258–268

# Darwin Spherical-Wave Theory of Kinematic Surface Diffraction

BY S. M. DURBIN

*Department of Physics, Purdue University, West Lafayette, IN* 47907, *USA*

(*Received* 5 *April* 1994; *accepted* 7 *September* 1994)

### Abstract

In 1912, von Laue first described X-ray diffraction by approximating as plane waves the spherical waves radiated by atoms in a crystal. Darwin recognized that this approximation is valid only in the limit of very small crystals, and published in 1914 the more general spherical-wave theory based on the reflectivity of individual atomic planes. The Darwin theory is extended here to surface Bragg diffraction from a single-crystalline